Altruistic Control of Connected Automated Vehicles in Mixed-Autonomy Multi-Lane Highway Traffic

Altruistic Control of Connected Automated Vehicles in Mixed-Autonomy Multi-Lane Highway Traffic

Musa Furkan Keskin * **Bile Peng** ** **Balazs Kulcsar** * **Henk Wymeersch** *

* *Department of Electrical Engineering, Chalmers University of Technology, SE-41296, Gothenburg, Sweden (e-mail: {furkan,kulcsar,henkw}@chalmers.se).*
** *Institute for Communications Technology, TU Braunschweig, (e-mail: bile.peng@gmail.com)*

Abstract: We consider the problem of altruistic control of connected automated vehicles (CAVs) on mixed-autonomy multi-lane highways to mitigate moving traffic jams resulting from car-following dynamics of human-driven vehicles (HDVs). In most of the existing studies on CAVs in multi-lane settings, vehicle controller design philosophy is based on a selfish driving strategy that exclusively addresses the ego vehicle objectives. To improve overall traffic smoothness, we propose an altruistic control strategy for CAVs that aims to maximize the driving comfort and traffic efficiency of both the ego vehicle and surrounding HDVs. We formulate the problem of altruistic control under a model predictive control (MPC) framework to optimize acceleration and lane change sequences of CAVs. In order to efficiently solve the resulting non-convex mixed-integer nonlinear programming (MINLP) problem, we decompose it into three non-convex subproblems, each of which can be transformed into a convex quadratic program via penalty based reformulation of the optimal velocity with relative velocity (OVRV) car-following model. Simulation results demonstrate significant improvements in traffic flow via altruistic CAV actions over selfish strategies on both single- and multi-lane roads.

Keywords: altruistic control, multi-lane highway, model predictive control, connected automated vehicles.

1. INTRODUCTION

Traffic jams on urban transportation networks pose a serious challenge towards safety, fuel economy and driving comfort. In dense traffic conditions, small disturbances due to accidents, closed lanes or random braking may amplify and propagate towards upstream as a result of car-following dynamics of human-driven vehicles (HDVs), leading to the so-called *moving traffic jams* [Sugiyama et al. (2008); Wang et al. (2016); Stern et al. (2018)]. To mitigate the effect of jamming waves on traffic flow, connected automated vehicle (CAV) based flow control approaches have become very popular in recent studies [Kamal et al. (2014, 2016); Wang et al. (2016); Stern et al. (2018)]. For single-lane scenarios, anticipative acceleration control can be used to ensure traffic smoothness by dissipating stop-and-go waves [Kamal et al. (2014); Dollar and Vahidi (2018); Stern et al. (2018)], while, for multi-lane highways, lane changing can be interpreted as a high-level strategic decision that can be optimized jointly with low-level acceleration inputs [Yu et al. (2019)].

In the literature, automated driving on multi-lane highways has usually been studied with an emphasis on the objectives of the host vehicle (i.e., CAVs) [Kamal et al. (2016); Bahram (2017); Yu et al. (2019)], ignoring the traffic-smoothing capabilities of CAVs [Stern et al. (2018)]. In [Kamal et al. (2016)], a driving strategy on multi-lane roads is proposed to increase the efficiency, comfort and safety of the host vehicle by optimization of acceleration and lane changes in a model predictive control (MPC) framework. However, the authors do not consider the objectives of the surrounding vehicles (i.e., *selfish driving*) and the impact of lane changing on attenuation of jamming waves. In [Bahram (2017)], an MPC-based mixed-integer quadratic programming problem is formulated to optimize longitudinal velocity and lane change maneuvers of the host vehicle. As another example of selfish driving, the study in [Yu et al. (2019)] develops a multi-agent reinforcement learning (RL) framework to achieve coordination among multiple automated vehicles on highways.

Unlike the previous research on CAV control in multi-lane traffic, in this study, we propose an *altruistic driving* strategy for CAVs to mitigate traffic jams on all lanes by considering the *objectives of the overall traffic*, i.e., both CAVs and surrounding HDVs. Altruistic driving has been considered only recently in several studies [Wang et al. (2017); Bıyık et al. (2018)]. In [Wang et al. (2017)], a cooperative altruistic driving strategy is developed to resolve traffic deadlocks on highways by forming a coordination group via vehicle-to-vehicle (V2V) communications among CAVs. The work in [Bıyık et al. (2018)] provides a game-theoretic analysis of altruistic autonomy from a routing

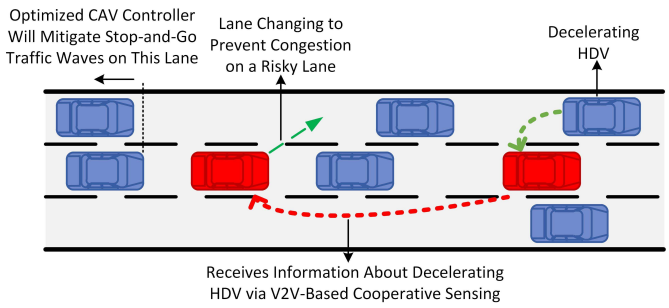

Fig. 1. Exemplary multi-lane highway scenario with CAVs (red) and HDVs (blue) where altruistic driving decisions of CAVs can help mitigate traffic jams and improve traffic smoothness (see Footnote 1 for details).

perspective and investigates its effect on traffic latency under varying degrees of altruism of CAVs. To the best of authors' knowledge, this is the first study to design altruistic CAV controllers on multi-lane roads with the key insight that altruistic lane change decisions of CAVs can help dissipate congestion waves and improve comfort and efficiency, as depicted in Fig. 1.

We propose an MPC based optimization approach to design altruistic driving strategies and incorporate the optimal velocity with relative velocity (OVRV) car-following model [Wilson and Ward (2011)] into our framework to predict future trajectories of HDVs. The resulting non-convex mixed-integer nonlinear programming (MINLP) problem is relaxed to convex quadratic programs. Simulation results reveal the benefits of the proposed altruistic control strategy over selfish driving.

2. SYSTEM MODEL

Consider a multi-lane highway with a mixed autonomy traffic containing both CAVs and HDVs, as shown in Fig. 1. We assume that each CAV obtains position and speed information of its surrounding HDVs via on-board sensors. Moreover, CAVs exchange locally observed vehicle information with one another in the communication range for the purpose of cooperative sensing [1] [Kim et al. (2015)]. In this scenario, the goal of each CAV is to determine optimal sequences of acceleration inputs and lane change decisions in an altruistic fashion to maximize traffic objectives of *all observable vehicles* (not only the ego vehicle).

2.1 Vehicle States

Let the state vector of the ith CAV at the discrete time instant k be defined as

$$\mathbf{x}_{i,k}^{\text{CAV}} = \left[p_{i,k}^{\text{CAV}} \;\; v_{i,k}^{\text{CAV}} \;\; y_{i,k}^{\text{CAV}}\right]^T \tag{1}$$

for $i = 1, \ldots, N_{\text{cav}}$, where $p_{i,k}^{\text{CAV}} \in \mathbb{R}$ and $v_{i,k}^{\text{CAV}} \in \mathbb{R}$ are, respectively, the longitudinal position and velocity of the vehicle, and $y_{i,k}^{\text{CAV}} \in \mathcal{L} \triangleq \{1, 2, \ldots, N_{\text{lane}}\}$ represents the lane number of the vehicle. Similarly, the state vector of the jth HDV at time k is expressed as

$$\mathbf{x}_{j,k}^{\text{HDV}} = \left[p_{j,k}^{\text{HDV}} \;\; v_{j,k}^{\text{HDV}} \;\; y_{j,k}^{\text{HDV}}\right]^T \tag{2}$$

for $j = 1, \ldots, N_{\text{hdv}}$, where $p_{j,k}^{\text{HDV}}, v_{j,k}^{\text{HDV}} \in \mathbb{R}$ and $y_{j,k}^{\text{HDV}} \in \mathcal{L}$.

[1] Here, we focus specifically on individual automated driving; thus, cooperation is used only for information sharing. Cooperative driving is outside the scope of this paper.

2.2 CAV Control Inputs

The control input vector of the ith CAV at time k is given by

$$\mathbf{u}_{i,k}^{\text{CAV}} = \left[a_{i,k}^{\text{CAV}} \;\; \delta_{i,k}^{\text{CAV}}\right]^T \tag{3}$$

where $a_{i,k}^{\text{CAV}} \in \mathbb{R}$ is the longitudinal acceleration and $\delta_{i,k}^{\text{CAV}}$ represents the lateral movement, i.e., the lane change decision, defined as

$$\delta_{i,k}^{\text{CAV}} \in \mathcal{L}_\Delta \triangleq \{-1, 0, 1\} \tag{4}$$

with 0 denoting the lane-keeping decision and -1(1) representing the lane-change-to-left (right) decision [2].

2.3 Car-Following Behavior of HDVs

To describe the longitudinal dynamics of HDVs, we use a car-following model $f(\cdot)$ as [Orosz et al. (2010)]

$$a_{j,k}^{\text{HDV}} = f(h_{j,k}^{\text{HDV}}, v_{j,k}^{\text{HDV}}, \Delta v_{j,k}^{\text{HDV}}) \tag{5}$$

where $a_{j,k}^{\text{HDV}} \in \mathbb{R}$ is the longitudinal acceleration of the jth HDV at time k, $h_{j,k}^{\text{HDV}}$ and $\Delta v_{j,k}^{\text{HDV}}$ are, respectively, the headway and velocity difference between the jth HDV and its preceding vehicle, written as

$$h_{j,k}^{\text{HDV}} = p_{j,k}^{\text{HDV,pre}} - p_{j,k}^{\text{HDV}} \;, \tag{6}$$

$$\Delta v_{j,k}^{\text{HDV}} = v_{j,k}^{\text{HDV,pre}} - v_{j,k}^{\text{HDV}} \;, \tag{7}$$

with $p_{j,k}^{\text{HDV,pre}}$ and $v_{j,k}^{\text{HDV,pre}}$ representing the position and speed of the vehicle preceding the jth HDV at time k on the same lane, which may itself be an HDV or a CAV depending on the current road configuration.

For the car-following function, we use the Optimal Velocity with Relative Velocity (OVRV) model [Wilson and Ward (2011)]

$$f(h, v, \Delta v) = \alpha(V(h) - v) + \beta \Delta v \tag{8}$$

where $V(h)$ is the piecewise-linear range policy function (which maps a given headway to a desired velocity), defined as [Zhang and Orosz (2016)]

$$V(h) = \left[\widetilde{V}(h)\right]_0^{v_{\max}}, \widetilde{V}(h) = v_{\max} \frac{h - h_{\min}}{h_{\max} - h_{\min}} \tag{9}$$

with $[v]_0^{v_{\max}} \triangleq \max(0, \min(v_{\max}, v))$, and α, β, $h_{\min}$, $h_{\max}$ and $v_{\max}$ are driver-dependent model parameters [3].

2.4 Discrete-Time Vehicle Dynamics

Given a fixed time step of Δt, discrete-time dynamics of the ith CAV can be expressed as

$$\mathbf{x}_{i,k+1}^{\text{CAV}} = \mathbf{A}\mathbf{x}_{i,k}^{\text{CAV}} + \mathbf{B}\mathbf{u}_{i,k}^{\text{CAV}} \tag{10}$$

where

$$\mathbf{A} = \begin{bmatrix} 1 & \Delta t & 0 \\ 0 & 1 & 0 \\ 0 & 0 & 1 \end{bmatrix}, \; \mathbf{B} = \begin{bmatrix} \Delta t^2/2 & 0 \\ \Delta t & 0 \\ 0 & 1 \end{bmatrix}. \tag{11}$$

Similarly, the dynamics of the jth HDV can be written as

$$\mathbf{x}_{j,k+1}^{\text{HDV}} = \mathbf{A}\mathbf{x}_{j,k}^{\text{HDV}} + \mathbf{B}\mathbf{u}_{j,k}^{\text{HDV}} \tag{12}$$

where the input is defined as

$$\mathbf{u}_{j,k}^{\text{HDV}} = \left[a_{j,k}^{\text{HDV}} \;\; \delta_{j,k}^{\text{HDV}}\right]^T. \tag{13}$$

[2] We assume an instant lane change model where lane changing is completed in a single time step.

[3] For the sake of simplicity in anticipatory optimization of CAV control inputs in (3), HDVs are assumed to keep the same lane over the prediction horizon [Kamal et al. (2016)], i.e., $\delta_{j,k+n}^{\text{HDV}} = 0$ for $n = 0, 1, \ldots, N_{\text{p}} - 1$, where N_{p} denotes the prediction horizon.

3. MPC FORMULATION FOR INDIVIDUAL ALTRUISTIC DRIVING

In this section, we focus on the problem of individual altruistic driving of a given CAV. We first provide constraints on CAV inputs/states in a multi-lane setting and then formulate the optimal CAV control problem in the MPC framework.

3.1 Constraints

To formulate the optimal CAV control problem, we impose the following constraints on vehicle inputs and states.

Acceleration Bounds Longitudinal acceleration inputs of CAVs are bounded as

$$a_{\min} \le a^{\text{CAV}}_{i,k+n} \le a_{\max}\ ,\ n = 0, 1, \ldots, N_{\text{p}} - 1. \tag{14}$$

Lateral Safety Constraints For a planned lane change maneuver at the nth prediction step (i.e., when $\left|\delta^{\text{CAV}}_{i,k+n}\right| = 1$), the ith CAV should keep a safe headway h_{safe} with the closest vehicles in the new lane, i.e.,

$$p^{\text{CAV,bg}}_{i,k+n} - p^{\text{CAV}}_{i,k+n} \ge h_{\text{safe}},\ p^{\text{CAV}}_{i,k+n} - p^{\text{CAV,sm}}_{i,k+n} \ge h_{\text{safe}} \tag{15}$$

where $p^{\text{CAV,bg}}_{i,k+n}$ and $p^{\text{CAV,sm}}_{i,k+n}$ represent the longitudinal positions of the vehicles on the new lane that are closest to the ith CAV at time $k+n$ with $p^{\text{CAV,bg}}_{i,k+n} \ge p^{\text{CAV}}_{i,k+n} \ge p^{\text{CAV,sm}}_{i,k+n}$.

Longitudinal Safety Constraints To avoid collisions, CAVs should keep a minimum headway from the preceding vehicle on the same lane [Kamal et al. (2014)]:

$$p^{\text{CAV,pre}}_{i,k+n} - p^{\text{CAV}}_{i,k+n} \ge h_{\min} + t_{\min} v^{\text{CAV}}_{i,k+n}\ ,\ n = 1, \ldots, N_{\text{p}} \tag{16}$$

where $p^{\text{CAV,pre}}_{i,k+n}$ is the position of the vehicle preceding the ith CAV at time $k+n$ and $t_{\min}$ denotes the minimum time headway.

3.2 Objectives

We pursue the following objectives for the proposed MPC based CAV control problem.

Traffic Efficiency Traffic efficiency objective can be defined as the problem of maintaining a desired velocity V^* for the ith CAV (the ego vehicle) and the observable HDVs:

$$\mathcal{J}^{\text{eff}}_i(\mathbf{u}^{\text{CAV}}_{i,k:k+N_{\text{p}}-1}) = \sum_{n=0}^{N_{\text{p}}-1} \left[(v^{\text{CAV}}_{i,k+n} - V^*)^2 + \kappa \sum_{j \in \mathcal{G}^{\text{HDV}}_{i,k}} (v^{\text{HDV}}_{j,k+n} - V^*)^2 \right] \tag{17}$$

where $\mathcal{G}^{\text{HDV}}_{i,k}$ is the index set of HDVs that are behind the ith CAV at time k and are observed by it [4], and κ is a constant factor that represents the *level of altruism*, i.e., how much CAV prioritizes the surrounding traffic with respect to its own driving objectives [5].

Driving Comfort Driving comfort is related to the magnitude of accelerations

$$\mathcal{J}^{\text{comf}}_i(\mathbf{u}^{\text{CAV}}_{i,k:k+N_{\text{p}}-1}) = \sum_{n=0}^{N_{\text{p}}-1} \left[\left(a^{\text{CAV}}_{i,k+n}\right)^2 + \kappa \sum_{j \in \mathcal{G}^{\text{HDV}}_{i,k}} \left(a^{\text{HDV}}_{j,k+n}\right)^2 \right] \tag{18}$$

where the dependency of HDV accelerations on CAV control inputs is through (5)–(7).

Overall Objective Function For the ith CAV, the overall objective function at time k over a horizon of length N_{p} can be written as

$$\mathcal{J}^{\text{tot}}_i(\mathbf{u}^{\text{CAV}}_{i,k:k+N_{\text{p}}-1}) = \mathcal{J}^{\text{eff}}_i(\mathbf{u}^{\text{CAV}}_{i,k:k+N_{\text{p}}-1}) + w\, \mathcal{J}^{\text{comf}}_i(\mathbf{u}^{\text{CAV}}_{i,k:k+N_{\text{p}}-1}) \tag{19}$$

where w is a predetermined constant that strikes a balance between efficiency and comfort objectives. In the MPC formulation, safety is taken into consideration as hard physical constraints through (15) and (16).

3.3 MPC Prediction Heuristics

We assume constant acceleration heuristics for prediction of the leading HDV trajectories [6]. Specifically, at time k, we have

$$a^{\text{HDV}}_{j,k+n} = \widehat{a}^{\text{HDV}}_{j,k},\ j \in \mathcal{F}^{\text{HDV}}_{i,k} \tag{20}$$

for $n = 0, 1, \ldots, N_{\text{p}} - 1$, where $\mathcal{F}^{\text{HDV}}_{i,k}$ is the index set of leading HDVs observed by the ith CAV and $\widehat{a}^{\text{HDV}}_{j,k}$ denotes the measured acceleration of the jth HDV at time k. To prevent negative velocities for $\widehat{a}^{\text{HDV}}_{j,k} < 0$ and large N_{p}, $a^{\text{HDV}}_{j,k+n}$ is set to zero for $n > \widetilde{n}$ if $v^{\text{HDV}}_{j,k+\widetilde{n}} < 0$. In other words, we prioritize speed constraint over (20) in the prediction horizon.

3.4 Problem Formulation

Given the initial states of the ith CAV and the HDVs observed by the ith CAV, the MPC optimization problem for the ith CAV at time k over N_{p} prediction steps can be stated as follows:

$$\begin{aligned} \underset{\mathbf{u}^{\text{CAV}}_{i,k:k+N_{\text{p}}-1}}{\text{minimize}}\ & \mathcal{J}^{\text{tot}}_i(\mathbf{u}^{\text{CAV}}_{i,k:k+N_{\text{p}}-1}) \\ \text{subject to}\ & \text{(Prediction of Leading HDVs) (20)} \\ & \text{(HDV Car-Following Model) (5)–(9)} \\ & \text{(CAV-HDV Dynamics) (10)–(13)} \\ & \text{(Vehicle/Traffic Constraints) (14)–(16)}\ . \end{aligned} \tag{21}$$

The problem in (21) is a challenging non-convex MINLP problem involving both continuous (acceleration sequence $a^{\text{CAV}}_{i,k:k+N_{\text{p}}-1}$) and discrete (lane change sequence $\delta^{\text{CAV}}_{i,k:k+N_{\text{p}}-1}$)

[4] The CAV can control only the vehicles behind (the so-called *Lagrangian control* [Stern et al. (2018)]) by using the state information of the vehicles both behind and in front for predictive optimization.

[5] We note that both CAV and HDV velocities in (17) depend on CAV control inputs $\mathbf{u}^{\text{CAV}}_{i,k:k+N_{\text{p}}-1}$ through (5)–(7) and (10). From the car-following behavior in (5)–(7), HDV acceleration is a function of the position and speed of the preceding vehicle, which implies that the effect of CAV control actions can be propagated upstream towards HDVs moving on the same lane and affect the traffic efficiency in (17).

[6] Since the accelerations of the leading HDVs on each lane cannot be determined using a car-following function as in (5), we assume that they are available (e.g., through tracking filters at CAVs) and therefore can be used for prediction of the future states of those HDVs.

variables (see (3)). The non-convexity of (21) results from the HDV longitudinal model in (5)–(7), which represents a non-convex piecewise-linear equality constraint.

4. OPTIMIZATION STRATEGIES FOR ALTRUISTIC DRIVING

In this section, we design optimization strategies for solving the individual altruistic driving problem in (21). We first reformulate the non-convex HDV car-following constraints into linear form. Subsequently, to handle the integer lane change variables, we decompose the original problem into several low-level subproblems for each lane, the solutions of which can then be combined to reach the optimal acceleration and lane change decisions.

4.1 Transformation of Piecewise-Linear Car-Following Constraints

To circumvent the intractability of the piecewise-linear constraint regarding the HDV longitudinal dynamics in (5)–(9), we employ a penalty based approach to transform the piecewise-linear equality constraint in (5) into a linear equality constraint and two linear inequality constraints, along with a penalty term in the objective. Specifically, the car-following dynamics constraint in (5) with the OVRV model in (8), given by

$$a^{\mathrm{HDV}}_{j,k+n} = \alpha(V(h^{\mathrm{HDV}}_{j,k+n}) - v^{\mathrm{HDV}}_{j,k+n}) + \beta\Delta v^{\mathrm{HDV}}_{j,k+n} \tag{22}$$

for $n = 0, 1, \ldots, N_{\mathrm{p}} - 1$ and $j \in \mathcal{H}^{\mathrm{HDV}}_{i,k}$, can equivalently be rewritten by introducing a slack variable $\boldsymbol{\gamma}_j = \begin{bmatrix}\gamma_{j,N_{\mathrm{p}}-1} \ldots \gamma_{j,0}\end{bmatrix}^T$ as follows[7]. First, we introduce a penalty term in the objective function of (21) as

$$\mathcal{J}^{\mathrm{tot}}_i(\mathbf{u}^{\mathrm{CAV}}_{i,k:k+N_{\mathrm{p}}-1}) + \lambda \sum_{j\in\mathcal{H}^{\mathrm{HDV}}_{i,k}} \left\|\boldsymbol{\gamma}_j\right\|^2 \tag{23}$$

where λ is a preset weight parameter that controls the tightness of car-following dynamics in (22). Secondly, we reformulate (22) as

$$a^{\mathrm{HDV}}_{j,k+n} = \alpha(\widetilde{V}(h^{\mathrm{HDV}}_{j,k+n}) - v^{\mathrm{HDV}}_{j,k+n}) + \beta\Delta v^{\mathrm{HDV}}_{j,k+n} + \gamma_{j,n} \tag{24}$$

$$a^{\mathrm{HDV}}_{j,k+n} \le \alpha(\widetilde{V}(h_{\max}) - v^{\mathrm{HDV}}_{j,k+n}) + \beta\Delta v^{\mathrm{HDV}}_{j,k+n} \tag{25}$$

$$a^{\mathrm{HDV}}_{j,k+n} \ge \alpha(\widetilde{V}(h_{\min}) - v^{\mathrm{HDV}}_{j,k+n}) + \beta\Delta v^{\mathrm{HDV}}_{j,k+n} \tag{26}$$

for $n = 0, 1, \ldots, N_{\mathrm{p}} - 1$ and $j \in \mathcal{H}^{\mathrm{HDV}}_{i,k}$. To see the equivalence between (22) (with the objective in (21)) and (24)–(26) (with the objective in (23)) as $\lambda \to \infty$, we note that when $h^{\mathrm{HDV}}_{j,k+n} \in [h_{\min}, h_{\max}]$, (22) is equivalent to (24)–(26) with $\gamma_{j,n} = 0$. For $h^{\mathrm{HDV}}_{j,k+n} \notin [h_{\min}, h_{\max}]$, the new objective in (23) would force $\gamma^2_{j,n}$ to be as small as possible to satisfy (24)–(26) simultaneously, which would render (22) and (24) almost equivalent. Fig. 2 illustrates the convergence of the reformulated model in (23)–(26) to the true model in (9) as λ increases.

4.2 Optimization Subproblem for Fixed Lane Change Decision

To deal with integer lane change variables in (21), we decompose it into three subproblems each corresponding to a fixed lane change decision $\delta^{\mathrm{CAV}}_{i,k} \in \mathcal{L}_\Delta$[8]. Hence, with the reformulation in (23)–(26), the MPC optimization subproblem of (21) for a given lane change decision can be written as follows:

$$\underset{a^{\mathrm{CAV}}_{i,k:k+N_{\mathrm{p}}-1},\{\boldsymbol{\gamma}_j\}}{\text{minimize}} \quad \mathcal{J}^{\mathrm{tot}}_i(\mathbf{u}^{\mathrm{CAV}}_{i,k:k+N_{\mathrm{p}}-1}) + \lambda \sum_{j\in\mathcal{H}^{\mathrm{HDV}}_{i,k}} \left\|\boldsymbol{\gamma}_j\right\|^2 \tag{27}$$

$$\begin{aligned}\text{subject to}\quad & \text{(Prediction of Leading HDVs) (20)}\\ & \text{(HDV Car-Following Model) (24)–(26)}\\ & \text{(CAV-HDV Dynamics) (10)–(13)}\\ & \text{(Vehicle/Traffic Constraints) (14)–(16)}\ .\end{aligned}$$

We note that (27) is a convex optimization problem with a convex quadratic objective and linear constraints, and thus can be solved efficiently using interior-point methods [Boyd and Vandenberghe (2004)]. The solutions of (27) for $\delta^{\mathrm{CAV}}_{i,k} \in \mathcal{L}_\Delta$ can be combined to obtain the optimal lane change decision and the corresponding acceleration sequence $a^{\mathrm{CAV}}_{i,k:k+N_{\mathrm{p}}-1}$ by choosing the one with the smallest cost $\mathcal{J}^{\mathrm{tot}}_i(\mathbf{u}^{\mathrm{CAV}}_{i,k:k+N_{\mathrm{p}}-1})$[9].

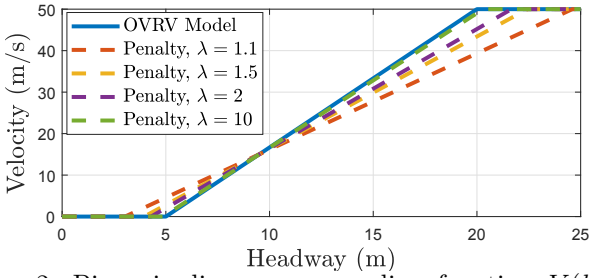

Fig. 2. Piecewise-linear range policy function $V(h)$ in (9) for the OVRV model compared against policy functions obtained through penalty based reformulation in (23)–(26), where $h_{\min} = 5\,\mathrm{m}$, $h_{\max} = 20\,\mathrm{m}$, $v_{\max} = 50\,\mathrm{m/s}$ and $\alpha = \beta = 2\,\mathrm{s}^{-1}$.

5. SIMULATION RESULTS

We present simulation results for both single-lane and multi-lane scenarios to verify the performance benefits of the proposed altruistic driving strategy. We compare three different controllers: *(i) No MPC*, where the CAV acts as an HDV, *(ii) Selfish CAV* with $\kappa = 0$, and *(iii) Altruistic CAV* with $\kappa > 0$. The simulation parameters are set as follows: $\alpha = \beta = 2\,\mathrm{s}^{-1}$, $h_{\min} = 2\,\mathrm{m}$, $h_{\max} = 20\,\mathrm{m}$, $v_{\max} = 50\,\mathrm{m/s}$, $N_{\mathrm{p}} = 80$, $\Delta t = 0.1\,\mathrm{s}$, $V^* = 30\,\mathrm{m/s}$, $a_{\min} = -10\,\mathrm{m/s^2}$, $a_{\max} = 10\,\mathrm{m/s^2}$, $h_{\mathrm{safe}} = 2\,\mathrm{m}$, $t_{\min} = 0\,\mathrm{s}$ and $w = 10\,\mathrm{s^2}$.

5.1 Single-Lane Road

We consider the single-lane scenario depicted in Fig. 3, where the leading HDV creates a sinusoidal disturbance corresponding to the acceleration profile as shown in

[7] $\mathcal{H}^{\mathrm{HDV}}_{i,k}$ is the index set of HDVs observed by the ith CAV, excluding the leading HDVs.

[8] This means that high-level lane change decisions are optimized in an unpredictive sense, considering only the current time instant, while low-level acceleration control inputs are obtained for N_{p} prediction steps forward in time. Intuitively, the algorithm tends to select the lane with the highest probability of congestion in the horizon (see Fig. 7 in Sec. 5.2 for an illustration).

[9] The optimization problem can either be solved on-board the ego vehicle or via cloud computing. For Python implementation with the parameters in Sec. 5, the solution time of each MPC cycle ranges from 1 s to 8 s, with an average of around 4 s.

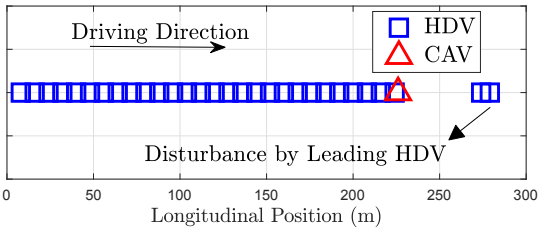

Fig. 3. Single-lane scenario with 30 HDVs and a CAV, where the leading HDV creates a sinusoidal disturbance pattern to mimic the impact of stop-and-go waves in dense traffic conditions.

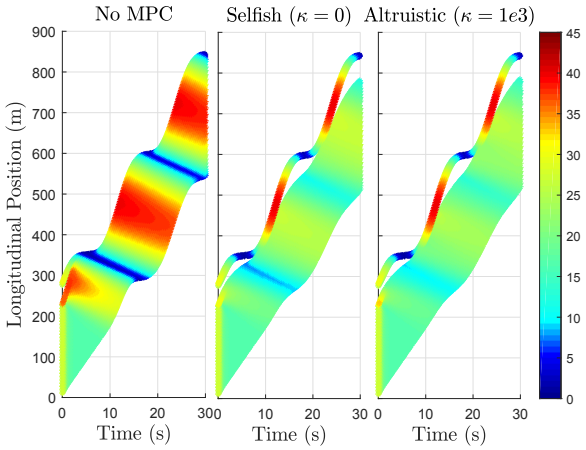

Fig. 4. Spatio-temporal trajectories corresponding to different driving strategies for the scenario in Fig. 3, where colors represent velocities (m/s^2). MPC strategy can smooth out stop-and-go waves - an effect that becomes more pronounced with higher degrees of altruism.

Fig. 6. The CAV is assumed to obtain the state information of the two HDVs in front and the four HDVs behind. In Fig. 4, we plot spatio-temporal trajectories for different driving strategies to illustrate their impact on traffic flow. It is observed that automated driving with the proposed MPC approach can dissipate stop-and-go waves and enhance traffic flow significantly, in compliance with the results in [Kamal et al. (2014); Wang et al. (2016); Stern et al. (2018)]. More importantly, altruistic driving can further improve overall traffic smoothness over selfish driving by taking into account the objectives of surrounding HDVs. This can also be seen from Fig. 5, where we observe reduced comfort and efficiency costs, and decreasing fluctuations in acceleration and velocity profiles as the level of altruism increases.

To investigate the quality of the approximation in Sec. 4.1, we plot, in Fig. 6, the predictive acceleration mismatch between reformulated OVRV model in (23)–(26) and original model in (22) during the altruistic driving scenario with $\kappa = 1e3$, averaged over all vehicles and the horizon. It is seen that the model mismatch is negligible except during periods of high HDV acceleration, for which the car-following model operates at extreme points where the model accuracy degrades, as illustrated in Fig. 2.

5.2 Multi-Lane Road

We consider the multi-lane scenario in Fig. 7, where traffic jam occurs on lane 3 due to disturbance by the leading HDV. For the altruistic strategy with $\kappa = 1e3$, we

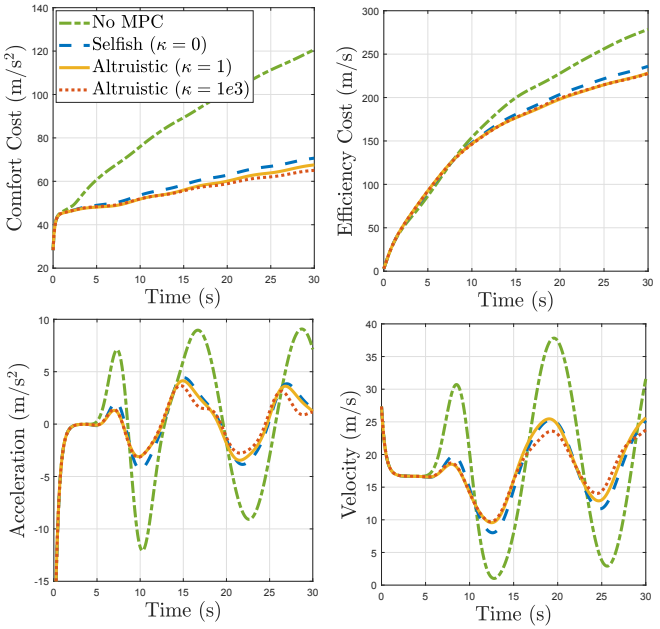

Fig. 5. (Top) Cumulative RMSE comfort and efficiency cost of all vehicles, and (Bottom) acceleration and velocity profiles of the 20th HDV, corresponding to different driving strategies for the scenario in Fig. 3.

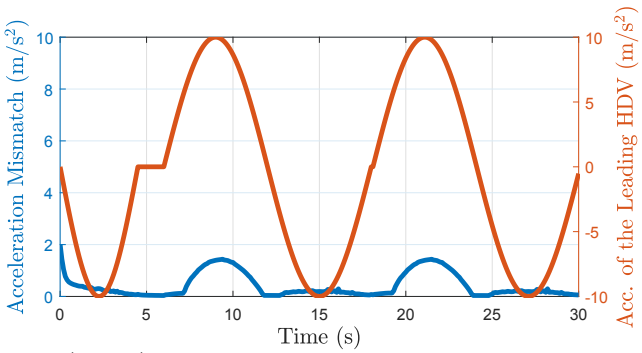

Fig. 6. (Right) Acceleration profile of the leading HDV vs. (Left) model mismatch between the predictive acceleration profile resulting from the reformulated model in (23)–(26) and that obtained by using the original HDV dynamics in (22).

observe that the CAV detects the presence of a jamming wave on lane 3 via predictive optimization and moves to that lane to dissipate congestion. However, the selfish CAV moves to lane 1 to maximize its own comfort and efficiency without considering the surrounding traffic. In Fig. 8, we plot acceleration magnitude profiles during the scenario corresponding to the selfish and altruistic strategies. It is observed that the altruistic CAV can substantially increase the driving comfort of all vehicles by applying harsh acceleration inputs (thus, sacrificing its own comfort) compared to the selfish CAV. As seen from Fig. 5 and Fig. 8, the benefits of altruistic driving are more pronounced in multi-lane traffic. This is because the behaviors of the CAV and the surrounding HDVs are tightly coupled in single-lane traffic while multiple lanes can offer higher degrees of freedom for performance improvement via altruism.

6. CONCLUSION

We have proposed an MPC based altruistic driving strategy for CAVs in a mixed-autonomy traffic to improve traf-

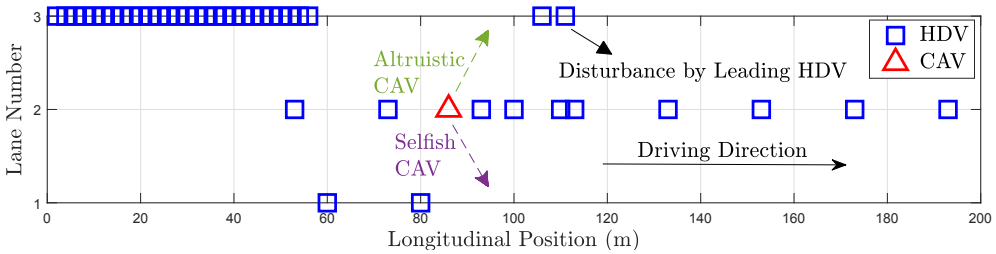

Fig. 7. Multi-lane scenario with 2 HDVs on lane 1, 10 HDVs and a CAV on lane 2, and 30 HDVs on lane 3, where the leading HDV on lane 3 creates a sinusoidal disturbance pattern that leads to a traffic jam. Given the acceleration of the leading HDV, an altruistic CAV would move to lane 3 to improve the traffic smoothness on that lane (also, the overall smoothness), while a selfish CAV would switch to lane 1 to maximize its own driving objectives.

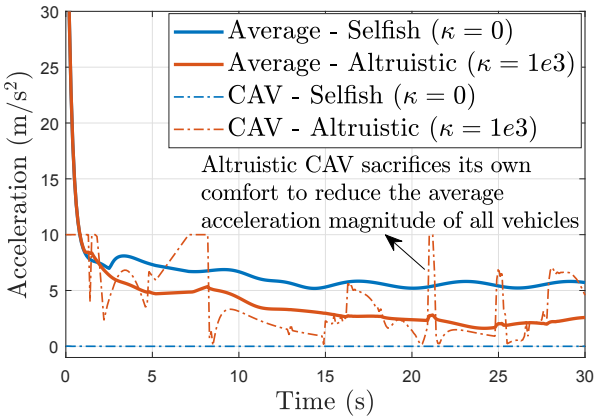

Fig. 8. Acceleration magnitude profiles for selfish and altruistic driving strategies in the scenario of Fig. 7.

fic flow. Simulation results have shown that the proposed altruistic driving approach can significantly outperform its selfish counterpart, especially on multi-lane roads. The future work will focus on cooperative altruistic driving with multiple CAV scenarios considering both centralized and distributed implementations.

ACKNOWLEDGEMENTS

This work is supported by Chalmers Transport Area of Advance and a SEED grant from the Department of Electrical Engineering, Chalmers University of Technology.

REFERENCES

Bahram, M. (2017). *Interactive Maneuver Prediction and Planning for Highly Automated Driving Functions*. Ph.D. thesis, Technische Universität München.

Bıyık, E., Lazar, D., Pedarsani, R., and Sadigh, D. (2018). Altruistic autonomy: Beating congestion on shared roads. *arXiv e-prints*, arXiv:1810.11978.

Boyd, S. and Vandenberghe, L. (2004). *Convex Optimization*. Cambridge university press.

Dollar, R.A. and Vahidi, A. (2018). Efficient and collision-free anticipative cruise control in randomly mixed strings. *IEEE Transactions on Intelligent Vehicles*, 3(4), 439–452. doi:10.1109/TIV.2018.2873895.

Kamal, M.A.S., Imura, J., Hayakawa, T., Ohata, A., and Aihara, K. (2014). Smart driving of a vehicle using model predictive control for improving traffic flow. *IEEE Transactions on Intelligent Transportation Systems*, 15(2), 878–888. doi:10.1109/TITS.2013.2292500.

Kamal, M.A.S., Taguchi, S., and Yoshimura, T. (2016). Efficient driving on multilane roads under a connected vehicle environment. *IEEE Transactions on Intelligent Transportation Systems*, 17(9), 2541–2551. doi:10.1109/TITS.2016.2519526.

Kim, S., Liu, W., Ang, M.H., Frazzoli, E., and Rus, D. (2015). The impact of cooperative perception on decision making and planning of autonomous vehicles. *IEEE Intelligent Transportation Systems Magazine*, 7(3), 39–50. doi:10.1109/MITS.2015.2409883.

Orosz, G., Wilson, R.E., and Stépán, G. (2010). Traffic jams: dynamics and control.

Stern, R.E., Cui, S., Monache, M.L.D., Bhadani, R., Bunting, M., Churchill, M., Hamilton, N., Haulcy, R., Pohlmann, H., Wu, F., Piccoli, B., Seibold, B., Sprinkle, J., and Work, D.B. (2018). Dissipation of stop-and-go waves via control of autonomous vehicles: Field experiments. *Transportation Research Part C: Emerging Technologies*, 89, 205 – 221. doi:https://doi.org/10.1016/j.trc.2018.02.005.

Sugiyama, Y., Fukui, M., Kikuchi, M., Hasebe, K., Nakayama, A., Nishinari, K., Tadaki, S.i., and Yukawa, S. (2008). Traffic jams without bottlenecks—experimental evidence for the physical mechanism of the formation of a jam. *New journal of physics*, 10(3), 033001.

Wang, M., Daamen, W., Hoogendoorn, S.P., and van Arem, B. (2016). Cooperative car-following control: Distributed algorithm and impact on moving jam features. *IEEE Transactions on Intelligent Transportation Systems*, 17(5), 1459–1471. doi:10.1109/TITS.2015.2505674.

Wang, N., Wang, X., Palacharla, P., and Ikeuchi, T. (2017). Cooperative autonomous driving for traffic congestion avoidance through vehicle-to-vehicle communications. In *2017 IEEE Vehicular Networking Conference (VNC)*, 327–330. doi:10.1109/VNC.2017.8275620.

Wilson, R.E. and Ward, J.A. (2011). Car-following models: fifty years of linear stability analysis–a mathematical perspective. *Transportation Planning and Technology*, 34(1), 3–18.

Yu, C., Wang, X., Xu, X., Zhang, M., Ge, H., Ren, J., Sun, L., Chen, B., and Tan, G. (2019). Distributed multiagent coordinated learning for autonomous driving in highways based on dynamic coordination graphs. *IEEE Transactions on Intelligent Transportation Systems*, 1–14. doi:10.1109/TITS.2019.2893683.

Zhang, L. and Orosz, G. (2016). Motif-based design for connected vehicle systems in presence of heterogeneous connectivity structures and time delays. *IEEE Transactions on Intelligent Transportation Systems*, 17(6), 1638–1651. doi:10.1109/TITS.2015.2509782.